Effects of heterocyclic ring and amino-ethyl-amino group on the electronic and photophysical properties of a triphenylamine-pyrimidine dye

Jieqiong Yang,[1] Dongzhi Liu,[1] Ting Lu,[1] Haiya Sun,[1] Wei Li,[1] Thomas T. Testoff,[2] Xueqin Zhou,[1] Lichang Wang[1,2]

[1]School of Chemical Engineering and Technology, Tianjin University, Tianjin 300354, China
[2]Department of Chemistry and Biochemistry and the Materials Technology Center, Southern Illinois University, Carbondale, IL 62901, United States

ABSTRACT

Introduction of a heterocyclic ring and an amino-ethyl-amino group to D-A type photosensitive dyes can modulate the lifetime of the charge separation generated in the D-A dyes as well as their electronic and UV-Vis absorption properties. Here we performed DFT and TDDFT calculations to study eleven derivatives of a triphenylamine-pyrimidine, MTPA-Pyc, in order to improve the performance of MTPA-Pyc as solar cell sensitizers. Five heterocyclic rings and an amino-ethyl-amino group were introduced on the styryl moiety of MTPA-Pyc. The results show that introduction of heterocyclic rings generally causes an absorption red-shift, but absorption intensity is reduced due to the increase of dihedral angle between the donor and acceptor. Further introduction of an amino-ethyl-amino group to these dyes with a heterocyclic ring modification disrupts the conjugation between donor and acceptor, which does not benefit the absorption but may have potential to increase the lifetime of charge separation of the dyes. This work identified two out of eleven dyes that have the best potential for solar cell applications.

1. INTRODUCTION

In recent years, with the increasing energy crisis, solar energy has received increasing attention as a renewable green energy source. As such, achieving highly efficient solar energy conversion has become a research hotspot. In the conversion from solar energy to electricity, charge separation is a critical step, which occurs either at the interface or soon after absorption of photons. In organic small molecule based dyes as sensitizers, the charge-transfer donor-acceptor (D-A) types of dyes tend to have charge separation taking place at the interface. While the D-A dyes with charge separated characteristics generate free charge carriers upon absorption of photons. For the charge separated D-A dyes, studies of the charge-separated state such as lifetime, have important applications in photocatalysts and solar cells.[1-10] As long-lived charge separated states show excellent performance in solar energy conversion, it is understandable that a lot of efforts have been invested in designing dyes with long-lived charge separation.

Two types of strategies have been used to increase the lifetime of charge separation. One is to design an architecture of D-A1-A2, i.e. bonding another acceptor to the acceptor of the D-A dye, so that the charge separated species can be further separated via electron transfer. For instance, 4,4'-dimethyl-4"-(4-(4-chloro-6-(2-(9,10-dioxoanthracen-1-ylamino)ethylamino)-1,3,5-triazin-2-ylamino)styryl)triphenylamine, denoted as MTPA-TRC-AEAQ, was designed using this principle. We showed that the life-time of MTPA-TRC-AEAQ was extended from 80 ns in triphenylamine-s-triazine (MTPA-TRC) to 650 ns by introducing anthraquinone as the second acceptor with an amino-ethyl-amino as the bridge between the two acceptors.[11] The second strategy to increase charge-separation lifetime is to modify the bridge between D-A dyes, which is the strategy that we will explore in this work. Using a triphenylamine-pyrimidine dye (denoted as MTPA-Pyc and shown in Figure 1), which shows promise in solar cell applications and has a charge separation lifetime of 64 ns,[12] we are interested in the effect of introducing various heterocyclic rings and an amino-ethyl-amino group on the electronic and photophysical properties and the lifetime of charge separation of the dyes.

Molecular design and further research on the photophysical properties of dyes through experimental synthesis and characterizations are extensive and time-consuming. Therefore, researchers have utilized theoretical calculations to prescreen candidates to assist experiments. At

present, density functional theory (DFT) and time-dependent density functional theory (TDDFT) are the most widely used methods in computational simulation of photophysical properties of organic small molecules and can predict and explain the properties of these molecules reasonably well.[13-20] For molecules with intramolecular charge transfer or charge separation, due to the complexity of the intramolecular electronic behavior, there may be discrepancies between the calculations and experiments, nonetheless, calculations still play an important role in molecular design and guiding experiments.[21-24] Therefore, in this work we used DFT and TDDFT calculations to prescreen candidates and study the effects of introducing various groups in the bridge of MTPA-Pyc on the electronic and photophysical properties of the dyes in order to select the best candidates to be tested in our future experiments.

The triphenylamine-pyrimidine dye, i.e. MTPA-Pyc shown in Figure 1, has a narrow absorption spectrum that is mainly located in the blue region. This is one of the main limiting factors for the application of this triphenylamine dye in organic solar cells. The photophysical properties of dye molecules can be improved by introducing different donor, acceptor, and π bridging groups, or by modifying the molecular structure with different substituents and heterocycles.[25-32] Since the heterocyclic ring has a good conjugation, the introduction of a heterocyclic ring between the donor and the acceptor can expand the conjugated structure of the dye molecule, adjust the orbital energy of the molecule, and improve the absorption spectrum of the dye.[33-36] The enhanced hyperconjugation between the donor and acceptor is disadvantageous for the separation of charges within the molecule and thus it is necessary to interrupt the interaction between the donor and the acceptor. Since non-conjugated chains can inhibit the back charge transfer and improve the charge separation efficiency of the D-A systems, the introduction of non-conjugated chains as a bridge between the donor and the acceptor has attracted widespread attention from researchers.[37-39] In addition to these heterocyclic groups, between the donor and acceptor of the triphenylamine-s-triazine binary electron transfer systems, non-conjugated alkyl-amino groups of different lengths were introduced. Studies illustrated that the systems after the introduction of non-conjugated chains indeed all show long-lived charge-separated states.[40]

Therefore, based on the charge-separated dye molecule MTPA-Pyc, we carried out DFT and TDDFT calculations on the dyes by introducing different heterocycles on the benzene ring in the styryl group and further introducing an amino-ethyl-amino group between the donor and the

acceptor. Specifically, we studied the ground state geometry, frontier molecular orbitals, and UV-Visible absorption spectra of the design dyes and compared these properties to provide the recommendation to the future experimental work.

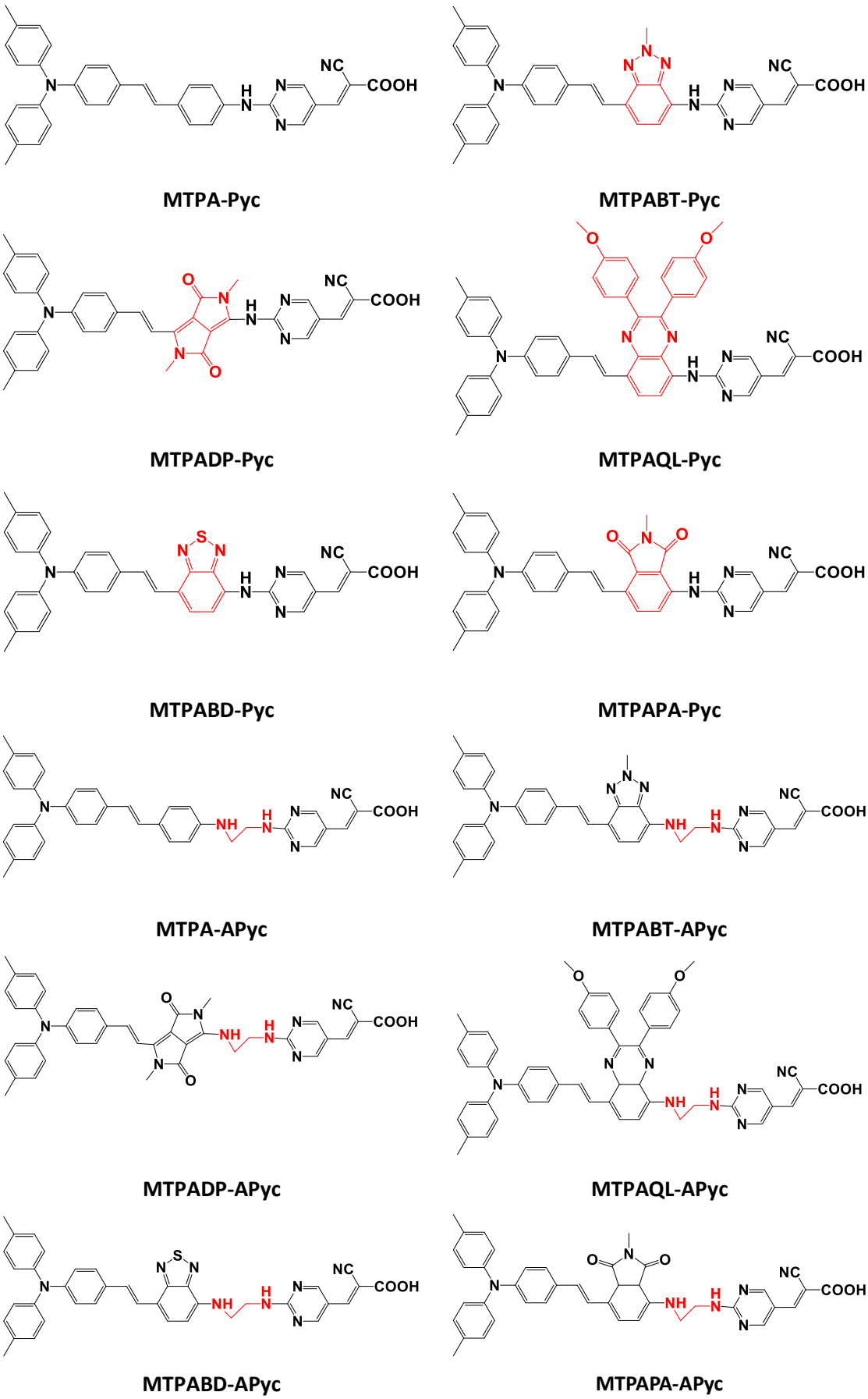

FIGURE 1 Heterocyclic and amino-ethyl-amino modified triphenylamine-pyrimidine dye structures

2. CALCULATION METHODS

All calculations in this work were performed using Gaussian 09 software. The ground state geometry optimizations of all 12 dye molecules shown in Figure 1 were performed at the B3LYP[41, 42]/6-31G (d, p) level. There were no restrictions on the symmetry of the molecules during the optimization. In order to consider the solvent effect, dichloromethane was chosen that was used in the experiment, and the solvent model was the Polarizable Continuum Model (PCM). Standard convergence criteria were used, i.e. the SCF, gradient, and energy convergence was set to be 10^{-8}, 10^{-4}, and 10^{-5} a.u., respectively. Frequency calculations were performed at the same theoretical level as geometry optimization and the results showed that all the optimized structures are at the minimum on the potential energy surface.

Using the optimized structures we performed TD-DFT calculations to obtain the absorption spectra of the lowest 50 single-excited states for the twelve dye molecules in dichloromethane. In the TD-DFT calculations, the range separation functional ωB97XD[43] was used and 6-311G(d,p) basis set[44-46] was used for all atoms. Note that our previous work showed that this basis set has a good balance between accuracy and computing time.[47]

3. RESULTS AND DISCUSSION

To study the effect of five heterocyclic rings and amino-ethyl-amino linker on the structure, electronic, and photophysical properties of MTPA-Pyc, we performed DFT and TDDFT calculations. The results on the structural changes are presented in section 3.1. The electronic properties, i.e. frontier orbital contours and energies, and the UV-Vis spectra of the molecules are presented in section 3.2 and 3.3, respectively.

3.1 Ground state geometries

Figure 2 summaries the optimized structures of the twelve dyes in dichloromethane.

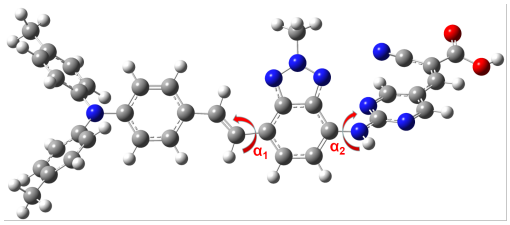

MTPABT-Pyc

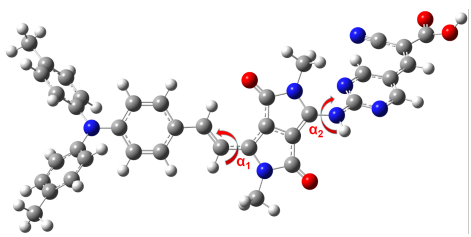

MTPADP-Pyc

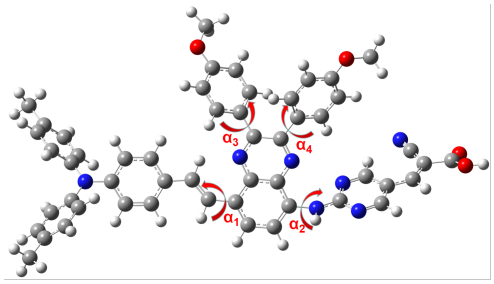

MTPAQL-Pyc

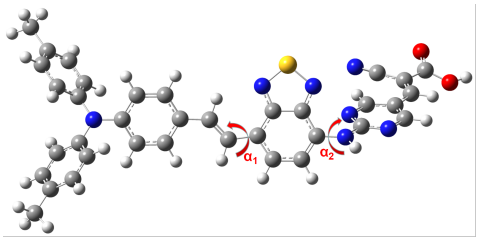

MTPABD-Pyc

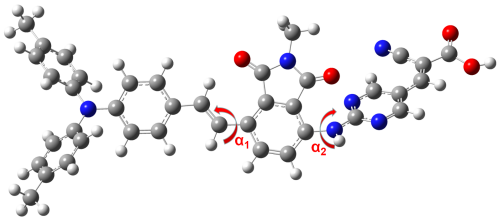

MTPAPA-Pyc

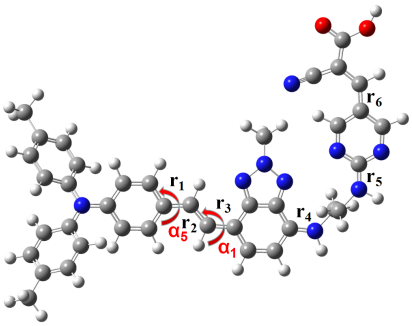

MTPABT-APyc

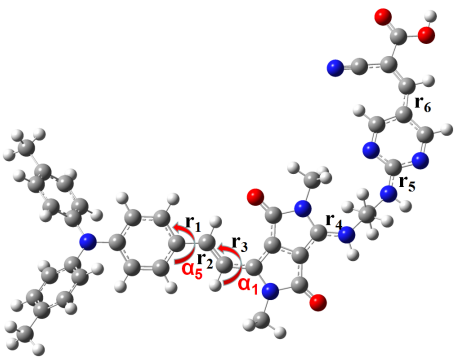

MTPADP-APyc

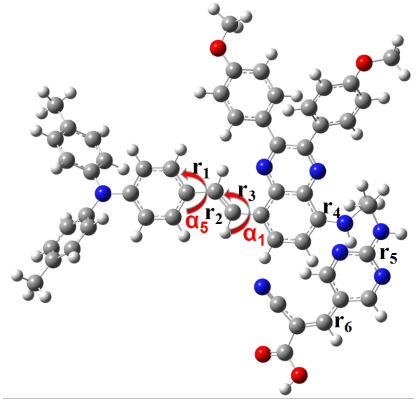

MTPAQL-APyc

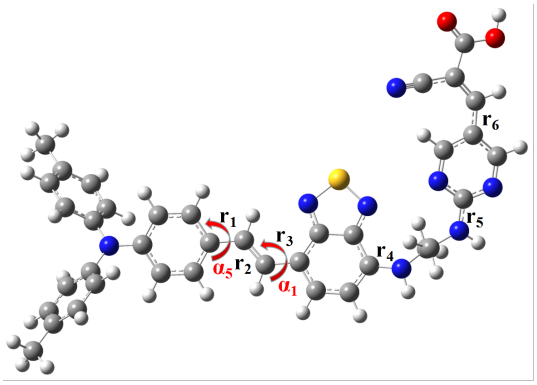

MTPABD-APyc

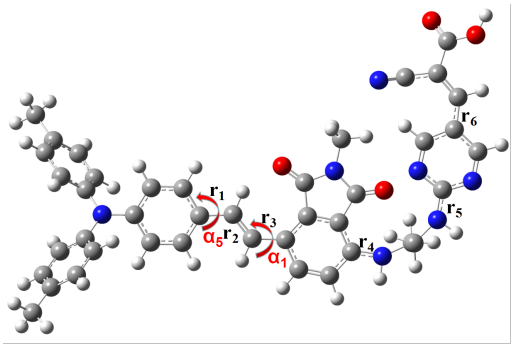

MTPAPA-APyc

FIGURE 2 The optimized structures of heterocyclic and amino-ethyl-amino modified dyes in dichloromethane. The grey, blue, red, yellow and white balls represent carbon, nitrogen, oxygen, sulfur and hydrogen atoms, respectively. Dihedral angles are α1, α2, α3 and α4 and bond lengths are r1, r2, r3, r4, r5 and r6.

As can be seen in Figure 2, after the introduction of the heterocycle, the donor moiety of the dye remains substantially planar except for the triphenylamine moiety. While the donor and acceptor exhibit distinct dihedral angles, in order to further illustrate the effect of the introduction of the heterocycle on the dye structure, we also listed in Table 1 the dihedral parameters of MTPABT-Pyc to MTPAPA-Pyc.

TABLE 1 Geometric parameters of heterocyclic modified dyes

	MTPABT-Pyc	MTPADP-Pyc	MTPAQL-Pyc	MTPABD-Pyc	MTPAPA-Pyc
α1 (°)	0.42	1.86	1.90	0.13	4.83
α2 (°)	50.51	35.59	59.87	55.17	48.21
α3 (°)			44.51		
α4 (°)			43.09		

In the dye molecule containing a heterocyclic ring, for the MTPAPA-Pyc molecule, the oxygen atom on the carbonyl group has a certain repulsion with the hydrogen atom on the vinyl group, therefore a small dihedral angle appears in the molecule. The heterocyclic rings in other dye molecules, although complex, do not have a substituent close to the hydrogen atom on the vinyl group, thus maintaining good planarity in the donor moiety. The MTPAQL-Pyc molecule has two larger substituted methoxyphenyl groups on the quinoxaline. These two substituents exhibit a dihedral angle of 44 degrees and 43 degrees with quinoxaline, respectively. Therefore, the structure of the entire molecule is distorted and the steric hindrance is large. The donor and acceptor moieties of all heterocyclic-containing dye molecules have a large dihedral angle, wherein the MTPABT-Pyc, MTPAPA-Pyc and MTPABD-Pyc molecules have a dihedral angle of about 50 degrees. In the MTPADP-Pyc molecule, the dihedral angle is small due to the small repulsion of the heterocyclic ring and the acceptor moiety. In MTPAQL-Pyc, since the heterocyclic structure is complicated and twisted at a certain angle, the steric hindrance between the heterocyclic ring and the acceptor moiety is large, so the dihedral angle is large. In summary, the introduction of the heterocycle destroys the planarity of the original molecule, weakens the interaction between the donor and the acceptor, and also affects the planarity of the donor moiety to some extent.

To interrupt the interaction between the receptors, we further inserted an amino-ethyl-amino group between the donor and acceptor of the dye. As can be seen from the optimized structure of Figure 2, the two methylene groups of the amino-ethyl-amino group in the dye are folded into a

cross-conformation such that the donor moiety and the acceptor moiety appear in two planes that are nearly parallel. In the dye molecule MTPAQL-APyc, due to the complicated structure of the heterocyclic moiety, the steric hindrance is large, and the acceptor moiety is folded down. After the introduction of the amino-ethyl-amino group, in order to further explore its influence on the dye structure and the interaction between the donor and the acceptor, we summarized some important bond length and dihedral data of the dyes into Table 2.

TABLE 2 Geometric parameters of dyes after introduction of amino-ethyl-amino

	MTPABT-APyc	MTPADP-APyc	MTPAQL-APyc	MTPABD-APyc	MTPAPA-APyc
r1 (Å)	1.462	1.452	1.463	1.462	1.461
r2 (Å)	1.354	1.362	1.354	1.354	1.354
r3 (Å)	1.452	1.434	1.460	1.454	1.462
r4 (Å)	1.382	1.358	1.386	1.382	1.384
r5 (Å)	1.346	1.346	1.345	1.346	1.346
r6 (Å)	1.436	1.438	1.436	1.436	1.436
α1 (°)	0.67	1.73	4.37	0.00	7.03
α5 (°)	176.74	179.53	174.17	179.12	174.3

After the introduction of amino-ethyl-amino group between donor and acceptor, the styryl moiety of MTPABT-APyc, MTPADP-APyc and MTPABD-APyc still showed good planarity, in MTPAQL-APyc and MTPAPA-APyc molecules, due to the more complex structure of the heterocyclic moiety, the steric hindrance is larger, and a small dihedral angle appears. It should be noted that although the donor moiety was modified with a different heterocycle, the bond length of the acceptor moiety was almost unchanged, indicating that the insertion of the amino-ethyl-amino group disrupted the interaction between the donor and the acceptor. This will facilitate the construction of charge-separated dyes.

3.2 Electronic properties

Figure 3 shows the electronic structure distribution of the pyrimidine series dyes frontier orbital.

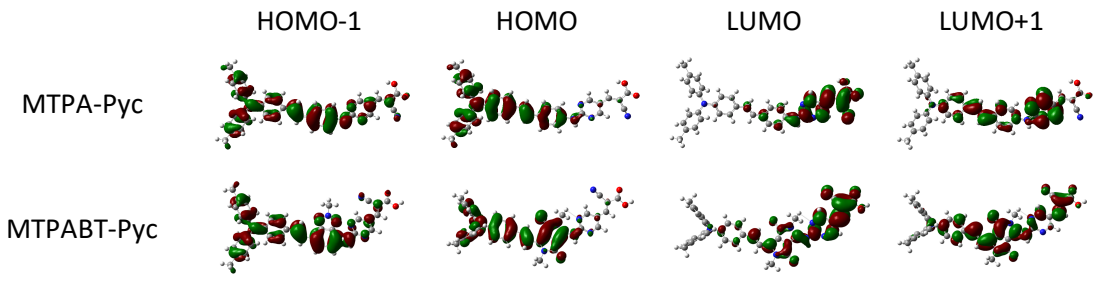

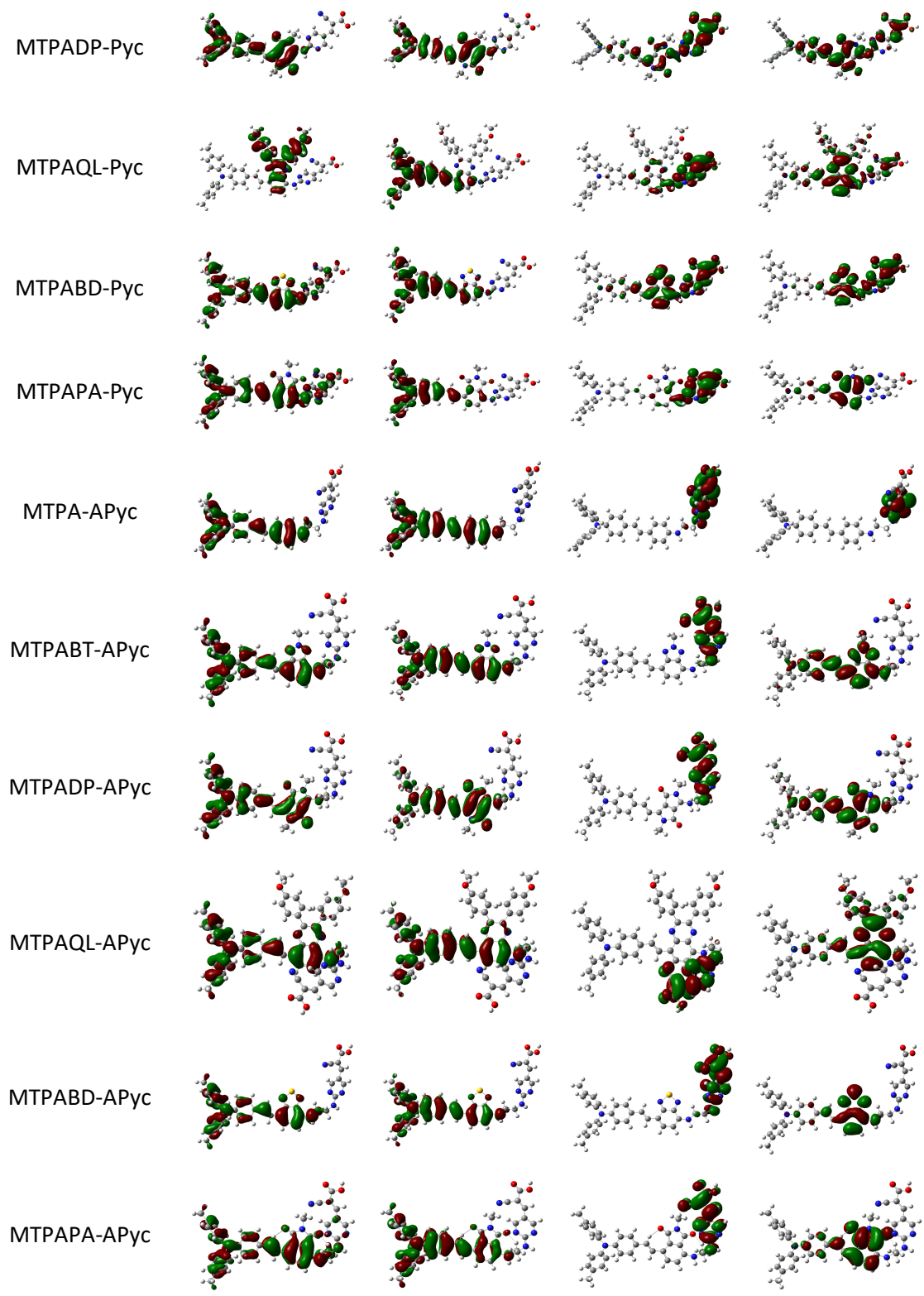

FIGURE 3 Molecular orbital contours of heterocyclic and amino-ethyl-amino modified dyes

It can be seen from Figure 3 that the frontier orbital distribution of MTPABT-Pyc containing heterocyclic benzotriazole is similar to that of the unmodified dye MTPA-Pyc. The HOMO-1 orbital is

delocalized throughout the dye molecule, the HOMO orbital is distributed only in the donor moiety, the LUMO orbital is mainly distributed in the acceptor moiety and has a small overlap with the HOMO orbital, and the LUMO+1 orbital is distributed throughout the molecule. Unlike the MTPA-Pyc molecule, the HOMO-1 of the MTPADP-Pyc molecule is only distributed in the donor moiety and is similar to the HOMO distribution region, while the LUMO is not only distributed on the acceptor but also extends to the benzene ring of the triphenylamine moiety. This makes the electron of the HOMO have a large overlap with the LUMO. Thus, in the MTPADP-Pyc molecule, the heterocyclic pyrrolopyrroledione is no longer a part of the donor, but acts as a π bridge connecting the donor to the acceptor to make the entire molecule a conjugate.

The most important difference between the electronic distribution of MTPAQL-Pyc and MTPA-Pyc is that the HOMO-1 of MTPAQL-Pyc is only distributed on the heterocyclic di-methoxy-phenyl-quinoxaline. Although the structure of the quinoxaline heterocycle is large, the coverage of the HOMO-LUMO orbital remains as small as that of MTPA-Pyc, indicating that the electronic structure of the MTPAQL-Pyc molecule has not changed substantially. The electron distribution of MTPABD-Pyc molecule is similar to that of MTPADP-Pyc. The LUMO covers almost the entire molecule, which makes the HOMO-LUMO orbital overlap increase, and the whole molecule exhibits the characteristics of intramolecular charge transfer. The HOMO-1, HOMO, and LUMO distributions of MTPAPA-Pyc molecules are also similar to MTPA-Pyc, but the HOMO-LUMO orbital overlap of MTPAPA-Pyc molecules is smaller than that of MTPA-Pyc molecules, and the LUMO+1 is only distributed in donor part. The orbital distribution of the MTPAPA-Pyc molecule will be more conducive to the intramolecular charge transfer of the donor moiety upon excitation and then further electron transfer to the acceptor moiety.

After the introduction of the heterocyclic ring, we further introduced an amino-ethyl-amino group between the donor and the acceptor. The aim is to completely break the conjugation between the donor and the acceptor and to reduce the overlap between the HOMO-LUMO to design a novel charge-separated dye. It can be seen in Figure 3 that after the introduction of amino-ethyl-amino group, the HOMO-1 and HOMO of the dye are only distributed in the donor moiety, the LUMO is only distributed in the acceptor moiety, and there is indeed no overlap between the HOMO and LUMO. The LUMO+1 of the dye molecules of MTPABT-APyc, MTPADP-APyc, MTPAQL-APyc, MTPABD-APyc, and MTPAPA-APyc is also only distributed in the donor moiety and concentrated in

the styryl-benzene ring moiety. The HOMO-1, HOMO, and LUMO+1 of the dyes are localized at the donor moiety, while the LUMO is by the acceptor moiety, with little or no electronic coupling between the donor and the acceptor. Therefore, when these dyes are excited, the HOMO electrons will mainly transition to the LUMO+1, the intramolecular charge transfer occurs in the donor moiety, and the electrons at the LUMO+1 orbital are further transferred to the LUMO orbital to form a charge-separated state.

It is worth noting that the LUMOs of MTPADP-Pyc and MTPABD-Pyc are distributed almost entirely throughout the molecule prior to the introduction of the amino-ethyl-amino group. There is no obvious boundary between the electron-donating group and the electron-withdrawing group, and the electron coupling is strong, making the whole molecule a conjugate. Upon introduction of the amino-ethyl-amino group, the conjugation between the donor and the acceptor is interrupted such that the heterocycle in the MTPADP-APyc and MTPABD-APyc molecules acts only as part of the donor and has no effect on the acceptor. Therefore there is no overlap between the HOMO and LUMO of the molecules.

To further understand the effect of the introduction of amino-ethyl-amino groups on the orbital energy of dye molecules, we plotted the orbital energy diagrams of the dyes in Figure 4.

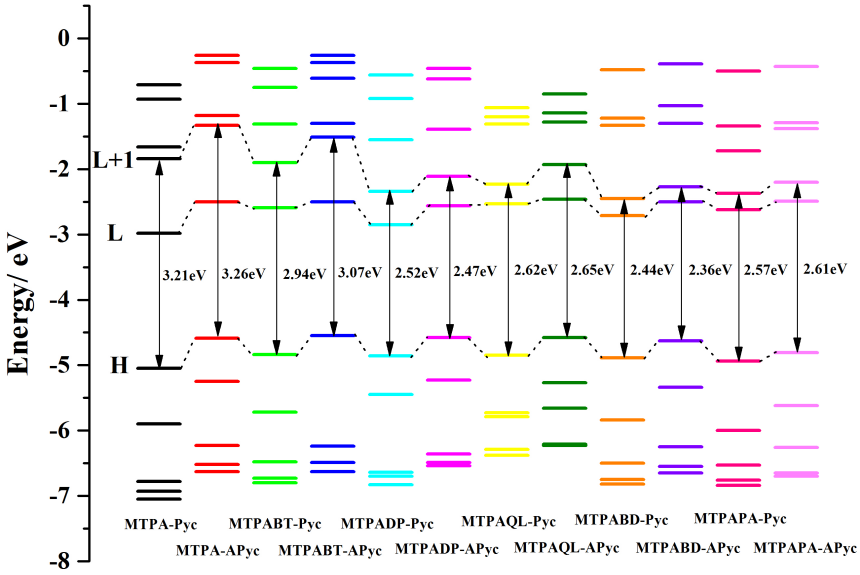

FIGURE 4 Molecular Orbital Energies of Heterocyclic and Amino-ethyl-amino Modified Dyes

After the introduction of the heterocyclic ring on the styryl-benzene ring, the degree of conjugation of the donor moiety is enlarged to some extent. On the other hand, the presence of

larger dihedral angles in the molecule weakens the interaction between the donor and the acceptor. Therefore, the HOMO energy of all the heterocyclic-containing dyes is overall higher than that of MTPA-Pyc. The LUMO energy also increases. The HOMO-LUMO energy gap of the MTPABT-Pyc molecule containing benzotriazole is larger than that of MTPA-Pyc, but the LUMO+1 energy decreases and the HOMO-LUMO+1 energy gap is reduced. The benzothiadiazole of MTPABD-Pyc molecule and the pyrrolopyrroledione of MTPADP-Pyc molecule as a π bridge blur the boundary between the donor and the acceptor, enhancing the interaction and making the whole molecule a conjugated system. The HOMO orbital energy level of the molecule increases, and the LUMO and LUMO+1 orbital levels decrease.

After the introduction of the heterocyclic ring, the LUMO+1 energies of MTPAQL-Pyc and MTPAPA-Pyc are significantly reduced and the HOMO energies were increased. Therefore, the HOMO-LUMO+1 orbital energy gap of the molecules are greatly changed compared with the MTPA-Pyc molecule, which is reduced by 0.77 eV and 0.64 eV, respectively. Therefore, after introduction of the heterocycle, in MTPABT-Pyc, MTPAQL-Pyc and MTPAPA-Pyc, the electron distribution of the frontier orbital does not change, so there is still significant charge separation. However, the energy of the frontier orbits have changed.

The introduction of the heterocycle not only raises the HOMO energy but also reduces the LUMO+1 energy, achieving bidirectional adjustment of the orbital energy level. This will further reduce the HOMO-LUMO+1 energy gap and increase its contribution at the maximum absorption peak. After the introduction of amino-ethyl-amino group, the energy levels of MTPABT-APyc to MTPAPA-APyc molecules increased, while the HOMO level of MTPADP-APyc and MTPABD-APyc increased more than the LUMO+1 level. Therefore, compared with the molecule without the amino-ethyl-amino group, the HOMO-LUMO+1 energy gap of the two molecules, MTDPDP-APyc and MTPABD-APyc, is reduced, which is beneficial to improve the absorption spectrum of the molecule.

3.3 UV-Vis absorption spectra

Figure 5 depicts the simulated absorption spectra of the dyes after introduction of a heterocyclic ring and further introduction of an amino-ethyl-amino group. As shown in Figure 5, the absorption of MTPABT-Pyc is slightly red shifted. The presence of methyl-benzotriazole effectively reduced the

LUMO+1 level, thereby reducing the energy gap of HOMO-LUMO+1 and causing the red shift in the absorption spectrum.

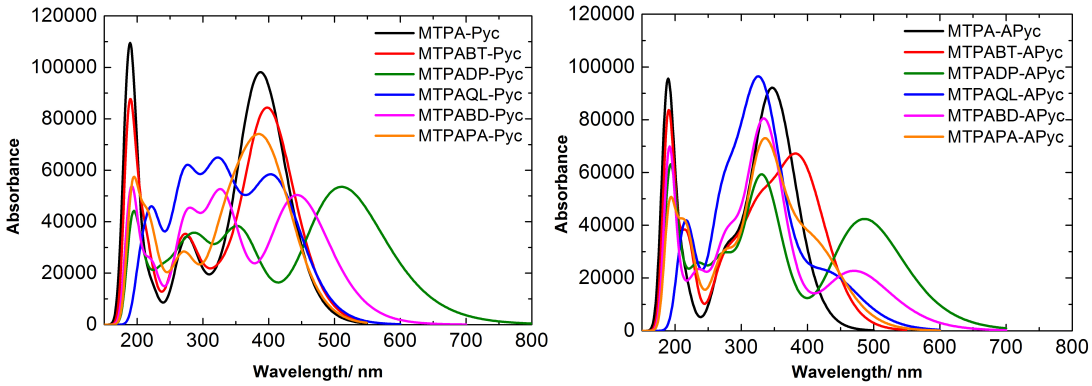

FIGURE 5 Simulated Absorption Spectrum of Heterocyclic and Amino-ethyl-amino Modified Dyes Obtained by ωB97XD/6-311G(d,p) Calculation in Dichloromethane

The MTPADP-Pyc molecule is a conjugate, so its maximum absorption peak position undergoes a significant red shift, and a new absorption peak appears, extending the absorption spectrum towards 800 nm. In the absorption spectrum of MTPAQL-Pyc molecule, a new absorption peak appeared near the maximum absorption peak, and the absorption intensity was higher than the maximum absorption peak, broadening the entire absorption spectrum, and the maximum absorption peak was red-shifted. The HOMO and LUMO of the MTPABD-Pyc molecule overlap to a greater extent, exhibiting the hyper-conjugation of the entire molecule, and thus its absorption spectrum has a significant red shift. The absorption spectrum of MTPAPA-Pyc molecule is similar to that of MTPABT-Pyc molecule in shape, but the maximum absorption peak is red-shifted and the absorption band is slightly wider. In summary, the absorption spectra of MTPADP-Pyc, MTPAQL-Pyc, and MTPABD-Pyc molecules all showed a new absorption peak near the maximum absorption peak, which broadened the absorption spectrum to some extent and improved the absorption characteristics of dye molecules.

After the introduction of amino-ethyl-amino group, the intensity of the maximum absorption peak of all dyes is lower than that of MTPA-Pyc, which will affect the light absorption efficiency of such dyes at the maximum absorption wavelength. However, the maximum absorption peaks of MTPADP-APyc, MTPAQL-APyc, MTPABD-APyc and MTPAPA-APyc molecules are significantly red-shifted compared with that of MTPA-Pyc.

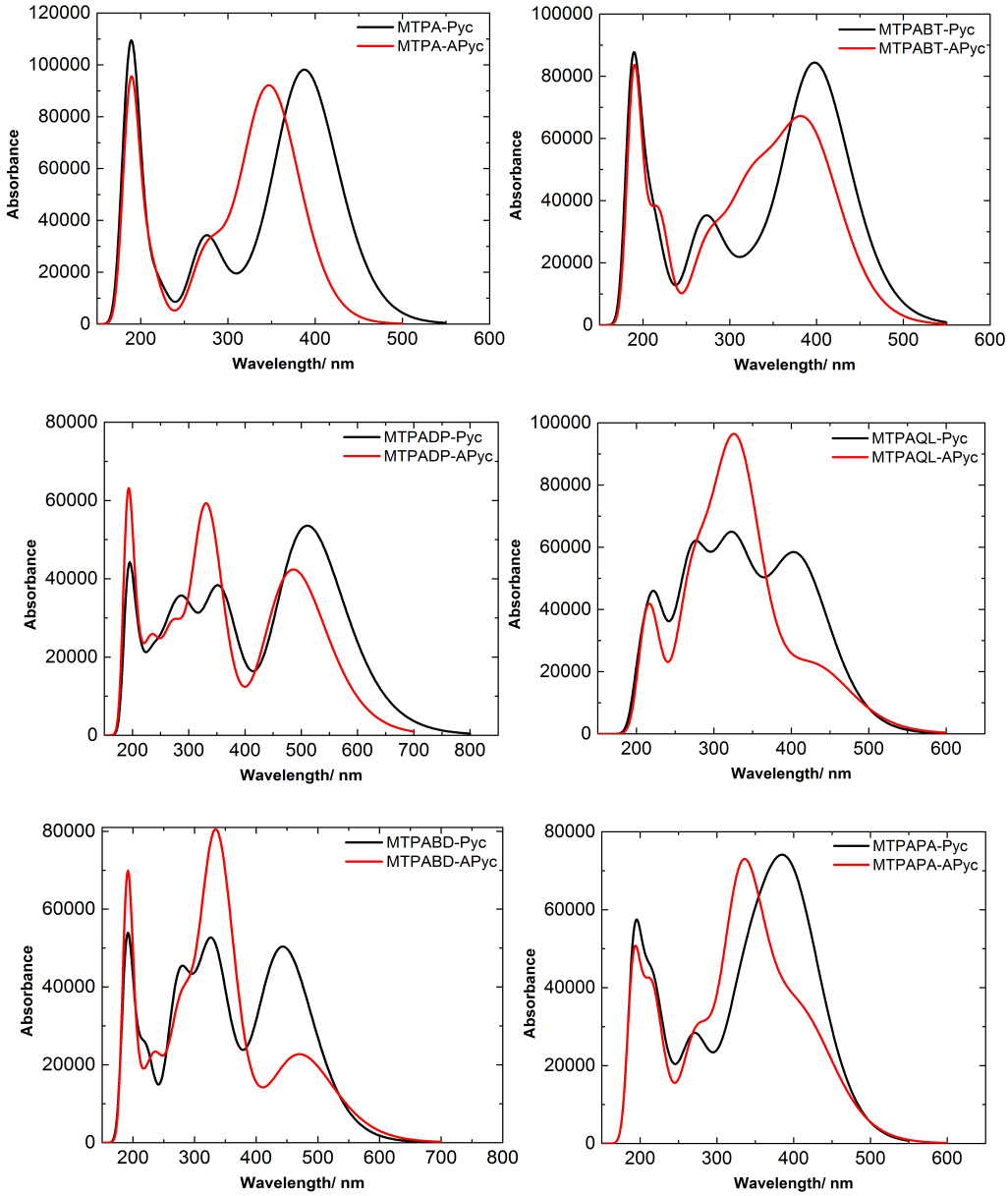

FIGURE 6 Comparative Simulation Absorption Spectra of Heterocyclic Modification and Aminoethylamino Introduction Obtained by ωB97XD/6-311G(d,p) Calculation in Dichloromethane

In Figure 6 we depicted the simulated absorption spectra of heterocyclic modification and amino-ethyl-amino inclusion to explore the influence of amino-ethyl-amino introduction on the absorption spectra of dye molecules. It can be seen in Figure 6 that the maximum absorption peak of MTPA-APyc molecule is significantly blue-shifted compared with MTPA-Pyc. However, since the second absorption peak and the maximum absorption peak are fused together to form a shoulder peak at the maximum absorption peak, the width of the absorption band is increased. The maximum absorption peak position of the MTPABT-APyc molecule is the same as that of the MTPA-APyc molecule, the absorption peak width is increased but the intensity is decreased compared with MTPABT-Pyc. The positions of the maximum absorption peaks of MTPAQL-APyc, MTPABD-APyc, and

MTPAPA-APyc molecules are significantly red-shifted after the introduction of aminoethylamino group, and the maximum absorption peaks of MTPADP-APyc and MTPABD-APyc molecules are red-shifted to around 500 nm. However, the intensity of the absorption peak is reduced, which is not conducive to the absorption of sunlight by the dye. Moreover, a second absorption peak with a large absorption intensity appears in the absorption spectra of MTPADP-APyc, MTPAQL-APyc, MTPABD-APyc and MTPAPA-APyc dye molecules.

TABLE 3 Calculated maximum absorption wavelength (λmax=nm), excitation energy (E),oscillator strengths (f) , light harvesting efficiency （LHE(λmax)） and electronic transition contributions of designed dyes in dichloromethane

Dyes	E/eV	λmax/nm	f	LHE(λmax)	contribution
MTPA-Pyc	3.18	390	2.346	0.995	H-1→L(25%) H→L(30%) H→L+1(26%)
MTPABT-Pyc	3.10	400	2.039	0.991	H-1→L(13%) H→L(23%) H→L+1(43%)
MTPADP-Pyc	2.43	511	1.321	0.952	H-1→L(8%) H→L(54%) H→L+1(31%)
MTPAQL-Pyc	3.03	409	1.352	0.956	H-2→L(13%) H→L(28%) H→L+1(34%)
MTPABD-Pyc	2.79	444	1.240	0.942	H-1→L(25%) H→L(51%) H→L+1(12%)
MTPAPA-Pyc	3.10	400	1.467	0.966	H-1→L(15%) H→L(7%) H→L+1(52%)
MTPA-APyc	3.45	360	1.441	0.964	H→L(4%) H→L+1(80%)
MTPABT-APyc	3.17	390	1.492	0.968	H-1→L+1(7%) H→L+1(81%)
MTPADP-APyc	2.55	486	1.046	0.910	H-1→L+1(4%) H→L(5%) H→L+1(87%)
MTPAQL-APyc	2.87	432	0.514	0.694	H-1→L+1(21%) H→L+1(72%)
MTPABD-APyc	2.63	471	0.559	0.724	H-1→L+1(24%) H→L(8%) H→L+1(62%)
MTPAPA-APyc	3.00	413	0.742	0.819	H-1→L+1(27%) H→L+1(63%)

In order to further analyze the orbital transitions at the maximum absorption peak, Table 3 lists the transition energy, oscillator strength, light absorption efficiency, and orbital transition contribution of the dyes. As the data shown in Table 3, the orbital transition contribution of the dye molecule has undergone a great change after the introduction of amino-ethyl-amino group. For MTPA-APyc, the contribution of the HOMO-LUMO+1 orbital transition accounts for 80% in the transition from the ground state to the first excited state, while the contribution of the HOMO-LUMO orbital transition is only 4%. It indicates that the transition is mainly the transition of electrons from the HOMO orbit to the LUMO+1 orbit. Such a transition mode is more conducive to the formation of a long-lived charge-separated state. However, due to the significant increase in the energy levels of HOMO, LUMO and LUMO+1 in the MTPA-APyc molecule, the HOMO-LUMO+1

energy gap is increased, so the maximum absorption peak is 30 nm blue shifted compared to MTPA-Pyc.

The orbital transition modes of MTPABT-APyc, MTPAQL-APyc and MTPAPA-APyc molecules are basically the same, mainly involving HOMO-LUMO+1 orbital transitions. At the same time, the MTPAQL-APyc and MTPAPA-APyc molecules have a large contribution to the HOMO-1-LUMO+1 orbital transition. Due to the different degree of regulation of orbital energy levels by different heterocycles, the maximum absorption peak positions of MTPABT-APyc and MTPAPA-APyc molecules are different, but they are significantly red-shifted compared with MTPA-APyc molecules. The maximum absorption peaks of MTPAQL-APyc and MTPAPA-APyc molecules were red-shifted to 432 nm and 413 nm, respectively.

When no amino-ethyl-amino group is introduced, the introduction of benzothiadiazole and pyrrolopyrroledione blurs the boundary between the donor and the acceptor, and the conjugation between the donor and the acceptor is enhanced. Therefore, the molecule becomes a charge-transfer type molecule, not a charge-separated type, and mainly occurs in the transition of the electron from the HOMO to the LUMO. After the introduction of the amino-ethyl-amino group, the benzothiadiazole and pyrrolopyrroledione in the MTPADP-APyc and MTPABD-APyc molecules only modified the donor moiety and had no effect on the acceptor moiety. The transition from the ground state to the first excited state is dominated by the HOMO-LUMO+1 transition, and the contribution of the HOMO-LUMO transition is significantly reduced. At the same time, benzothiadiazole and pyrrolopyrroledione have a greater effect on the bidirectional regulation of orbital energy levels. Therefore, the maximum absorption peaks of MTPADP-APyc and MTPABD-APyc dyes showed a significant red shift, which was red shifted to 487 nm and 471 nm, respectively.

4. CONCLUSIONS

We have performed theoretical studies on the effects of heterocyclic and amino-ethyl-amino groups on the electronic and photophysical properties of D-A triphenylamine dyes using DFT and TD-DFT calculations. The introduction of a heterocyclic ring on the styryl-benzene ring of the MTPA-Pyc dye leads to a large dihedral angle between the donor and the acceptor, which weakens the electronic coupling between the donor and the acceptor. The HOMO-LUMO overlap of the dyes,

MTPABT-Pyc, MTPAQL-Pyc, and MTPAPA-Pyc, is small, while the LUMOs of MTPADP-Pyc and MTPABD-Pyc molecules cover almost the entire molecule, making the whole molecule exhibit intramolecular charge transfer characteristics. The MTPABT-Pyc, MTPAQL-Pyc and MTPAPA-Pyc dyes not only raise the HOMO orbital energy level, but also lower the LUMO+1 energy level, achieving bidirectional regulation of the orbital energy level. The absorption spectra of the heterocyclic modified dyes were red-shifted, and the HOMO-LUMO+1 transition contributions of the MTPABT-Pyc and MTPAPA-Pyc dyes were significantly increased.

Further incorporating the amino-ethyl-amino group in the dyes completely interrupts the conjugation between the donor and the acceptor moieties, so that the donor moiety and the acceptor moiety become relatively independent parts. The HOMO-1, HOMO, and LUMO+1 of the dye are all distributed round the donor moiety, while the LUMO is distributed around the acceptor moiety. As such, there is no overlap between the HOMO and LUMO. The transition from the ground state to the first excited state is dominated by the HOMO to LUMO+1 transition. First, the intramolecular charge transfer of the donor moiety occurs, and further electron transfer occurs to form a charge separation state. Among them, the maximum absorption peaks of MTPADP-APyc, MTPAQL-APyc, MTPABD-APyc, and MTPAPA-APyc molecules are significantly red-shifted compared with MTPA-Pyc. Moreover, a second absorption peak with a large absorption intensity appears in the absorption spectra of MTPADP-APyc, MTPAQL-APyc, MTPABD-APyc, and MTPAPA-APyc molecules, which has a great application prospect for solar cells. Furthermore, this work suggests that MTPADP-APyc and MTPADP-Pyc are worth of first investigating experimentally.

ACKNOWLEDGEMENT

This work was supported by the National Nature Science Foundation of China NSFC (Grant No. 21776207 and 21576195).

REFERENCES

1. H. Ou, X. Chen, L. Lin, Y. Fang and X. Wang, *Angew Chem Int Ed Engl*, 2018, **57**, 8729-8733.
2. A. R. Artem A. Bakulin, Vlad G. Pavelyev, Paul H. M. van Loosdrecht, Maxim S. Pshenichnikov, Dorota Niedzialek, Jérôme Cornil, David Beljonne and Richard H. Friend, *Science*, 2012, **335**, 1340-1344.
3. G. Sini, M. Schubert, C. Risko, S. Roland, O. P. Lee, Z. Chen, T. V. Richter, D. Dolfen, V. Coropceanu, S. Ludwigs, U. Scherf, A. Facchetti, J. M. J. Fréchet and D. Neher, *Advanced Energy Materials*, 2018, **8**.
4. S. Yu, J. Li, Y. Zhang, M. Li, F. Dong, T. Zhang and H. Huang, *Nano Energy*, 2018, **50**, 383-392.

5. H. Huang, S. Tu, C. Zeng, T. Zhang, A. H. Reshak and Y. Zhang, *Angew Chem Int Ed Engl*, 2017, **56**, 11860-11864.
6. T. Wei, Y.-N. Zhu, Z. Gu, X. An, L.-m. Liu, Y. Wu, H. Liu, J. Tang and J. Qu, *Nano Energy*, 2018, **51**, 764-773.
7. S. Yin, R. Chen, M. Ji, Q. Jiang, K. Li, Z. Chen, J. Xia and H. Li, *Journal of colloid and interface science*, 2020, **560**, 475-484.
8. Q. Guo, J. Zhao, Y. Yang, J. Huang, Y. Tang, X. Zhang, Z. Li, X. Yu, J. Shen and J. Zhao, *Journal of colloid and interface science*, 2020, **560**, 359-368.
9. W. Huo, T. Cao, W. Xu, Z. Guo, X. Liu, H.-C. Yao, Y. Zhang and F. Dong, *Chinese Journal of Catalysis*, 2020, **41**, 268-275.
10. X. Fan, K. Lai, L. Wang, H. Qiu, J. Yin, P. Zhao, S. Pan, J. Xu and C. Wang, *J. Mater. Chem. A*, 2015, **3**, 12179-12187.
11. T. Wang, K. C. Weerasinghe, D. Liu, W. Li, X. Yan, X. Zhou and L. Wang, *J. Mater. Chem. C*, 2014, **2**, 5466-5470.
12. H. Sun, D. Liu, T. Wang, T. Lu, W. Li, S. Ren, W. Hu, L. Wang and X. Zhou, *ACS Appl Mater Interfaces*, 2017, **9**, 9880-9891.
13. V. Mohankumar, P. Pounraj, M. S. Pandian and P. Ramasamy, *Journal of Molecular Structure*, 2019, **1195**, 494-505.
14. L. Lyu, P. Tang, G. Tong and L. Han, *Journal of the Iranian Chemical Society*, 2019, **16**, 2441-2450.
15. Y. Kusumawati, A. L. Ivansyah, M. A. Martoprawiro, L. W. Oktavia, K. A. Madurani and F. Kurniawan, *Chiang Mai Journal of Science*, 2019, **46**, 1219-1228.
16. C. Fonkem, G. W. Ejuh, F. T. Nya, R. A. Y. Kamsi and J. M. B. Ndjaka, *Journal of the Iranian Chemical Society*, 2019, DOI: 10.1007/s13738-019-01790-4.
17. K. Paredes-Gil, D. Paez-Hernandez, R. Arratia-Perez and F. Mendizabal, *International Journal of Quantum Chemistry*, 2019, DOI: 10.1002/qua.26108.
18. I. Erden, A. Hatipoglu, C. Cebeci and S. Aydogdu, *Journal of Molecular Structure*, 2020, **1201**.
19. G. Deogratias, N. Seriani, T. Pogrebnaya and A. Pogrebnoi, *Journal of molecular graphics & modelling*, 2020, **94**, 107480-107480.
20. A. Slimi, A. Fitri, A. T. Benjelloun, S. Elkhattabi, M. Benzakour, M. McHarfi and M. Bouachrine, *Journal of Electronic Materials*, 2019, **48**, 4452-4462.
21. R. M. Richard and J. M. Herbert, *J Chem Theory Comput*, 2011, **7**, 1296-1306.
22. Q.-Q. Pan, Z.-W. Zhao, Y. Wu and Y. Geng, *Journal of molecular graphics & modelling*, 2020, **94**, 107488-107488.
23. F. Philippi, D. Rauber, M. Springborg and R. Hempelmann, *J Phys Chem A*, 2019, **123**, 851-861.
24. M. E. McCarroll, Y. Shi, S. Harris, S. Puli, I. Kimaru, R. Xu, L. Wang and D. J. Dyer, *J. Phys. Chem. B*, 2006, **110**, 22991-22994.
25. S. S. M. Fernandes, M. C. R. Castro, I. Mesquita, L. Andrade, A. Mendes and M. M. M. Raposo, *Dyes and Pigments*, 2017, **136**, 46-53.
26. L. Lyu, P. Tang, G. Tong and L. Han, *Journal of the Iranian Chemical Society*, 2019, **16**, 2441-2450.
27. K. Zeng, W. Tang, C. Li, Y. Chen, S. Zhao, Q. Liu and Y. Xie, *Journal of Materials Chemistry A*, 2019, **7**, 20854-20860.
28. M. M. Morgan, M. Nazari, T. Pickl, J. M. Rautiainen, H. M. Tuononen, W. E. Piers, G. C. Welch and B. S. Gelfand, *Chem Commun (Camb)*, 2019, **55**, 11095-11098.
29. G. Deogratias, N. Seriani, T. Pogrebnaya and A. Pogrebnoi, *Journal of Molecular Graphics and*

Modelling, 2020, **94**.

30. O. S. Al-Qurashi, N. A. Wazzan and I. B. Obot, *Molecular Simulation*, 2019, DOI: 10.1080/08927022.2019.1668561, 1-13.
31. Y. Xie, H. Zhou, S. Zhang, C. Ge and S. Cheng, *Photochemical & Photobiological Sciences*, 2019, **18**, 2042-2051.
32. A. Slimi, A. Fitri, A. Touimi Benjelloun, S. Elkhattabi, M. Benzakour, M. McHarfi and M. Bouachrine, *Journal of Electronic Materials*, 2019, **48**, 4452-4462.
33. Z. Yang, C. Liu, C. Shao, X. Zeng and D. Cao, *Nanotechnology*, 2016, **27**, 265701.
34. K. Stalindurai, A. Karuppasamy, J.-D. Peng, K.-C. Ho and C. Ramalingan, *Electrochimica Acta*, 2017, **246**, 1052-1064.
35. Y. K. Eom, S. H. Kang, I. T. Choi, Y. Yoo, J. Kim and H. K. Kim, *Journal of Materials Chemistry A*, 2017, **5**, 2297-2308.
36. H. Liu, B. Li, B. Xue and E. Liu, *Journal of Physical Chemistry C*, 2019, **123**, 26047-26056.
37. Y. T. Higashino T, Yamamoto M, Furube A, Tkachenko NV, Miura T, Kobori Y, Jono R, Yamashita K, Imahori H, *Angewandte Chemie International Edition*, 2016, **55**, 629-633.
38. T. H. Tomokazu Umeyama, Jinseok Baek, Tomohiro Higashino, Fawzi Abou-Chahine, Nikolai Tkachenko, Hiroshi Imahori, *The Journal of Physical Chemistry C*, 2016, **120**, 28337-28344.
39. T. Wang, C. Zhao, L. Zhang, T. Lu, H. Sun, C. N. Bridgmohan, K. C. Weerasinghe, D. Liu, W. Hu, W. Li, X. Zhou and L. Wang, *The Journal of Physical Chemistry C*, 2016, **120**, 25263-25275.
40. L. Pingan, Z. Xueqin, X. Jiaxuan, L. Dongzhi, L. Wei and W. Tianyang, *FINE CHEMICALS*, 2018, **35**, 1801-1816.
41. A. D. Becke, 1988, **38**, 3098-3100.
42. C. Lee, W. Yang and R. G. Parr, 1988, **37**, 785-789.
43. J. D. Chai and M. J. P. C. C. P. P. Head-Gordon, **10**, 6615-6610.
44. M. J. Frisch, J. A. Pople and J. S. J. J. o. C. P. Binkley, **80**, 3265.
45. R. Krishnan, J. S. Binkley, R. Seeger and J. A. Pople, *The Journal of Chemical Physics*, 1980, **72**, 650-654.
46. G. S. C. A. D. McLean, *J. Chem. Phys.*, 1980, **72**, 5639-5648.
47. G. A. Hudson, L. Cheng, J. Yu, Y. Yan, D. J. Dyer, M. E. McCarroll and L. Wang, *J. Phys. Chem. B*, 2010, **114**, 870-876.

Keywords: triphenylamine; pyrimidine; density functional theory (DFT); UV-Vis absorption; Electronic structure

TOC: